Progress In Electromagnetics Research, PIER 69, 237–246, 2007

TRANSPARENCY OF A PAIR OF EPSILON-NEGATIVE SLAB AND MU-NEGATIVE SLAB

X.-W. Dai, M. Yao, X.-J. Dang, and C.-H. Liang

National Key Laboratory of Antennas and Microwave Technology
Xidian University
Xi'an 710071, China

Abstract—Pairing an epsilon-negative (ENG) slab with a mu-negative (MNG) slab can have some unusual features, such as zero reflection and complete tunneling without any phase delay, although each of those two slabs has predicable features. In this paper, the conditions of zero reflection are obtained through an exact analysis, not by the equivalent transmission-line (TL) models. The distributions of fields and Poynting vector outside and inside such paired slabs are analyzed, while evanescent waves also are studied. Simulation results validate the salient features of such paired slabs.

1. INTRODUCTION

In recent years, metamaterial with negative permittivity or/and negative permeability has attracted a great deal of attention in many scientific disciplines. This dates back to 1960s when Veselago first introduced the concept of left-handed material (LHM) with simultaneously negative permittivity and negative permeability and anticipated their unique electromagnetic properties in theory [1]. But until 2001, the first artificial LHM composed of thin wire cylinder and split-ring resonators (SRR) was realized by Smith et al. [2], inspired by the work of J. B. Pendry [3]. Due to its salient features, many potential applications have been proposed and studied by many research groups, such as antennas [5, 6], phase shifters [7], filters [8], couplers [9, 10], etc.

Most of the work reported in recent literature has been focused not only on the media with two negative constitutive parameters, but also on the media with one negative constitutive parameter, like the media with negative permittivity or negative permeability [11]. It is well known that the electromagnetic wave can not propagate in ENG media or MNG media, however, when ENG slab and MNG slab are

paired in a conjugate manner, some unusual features are exhibited. Andrea Alù and Nader Engheta [12] have given the condition of conjugate matching, and shown that such a combination can provide the characteristics of resonance, complete tunneling and transparency, using the equivalent TL modes.

In this paper, the conditions of zero reflection for two layers are introduced first. Then the conditions of the transparency characteristic for a pair of ENG slab and MNG slab are carried through a strict calculation, not by the equivalent transmission-line (TL) models. The field distributions of propagating waves and the Poynting vector outside and inside such paired slabs are analyzed, which shows the unique features of a pair of ENG slab and MNG slab. Propagating waves can propagate through the paired slabs without any reflection and phase delay, as well as evanescent waves. Numerical experiments validate the above conclusions.

2. GENERAL GEOMETRY AND FORMULATION OF THE PROBLEM

First we consider a two-dimensional (2D) geometry shown in Fig. 1, all quantities are independent of the x coordinate. The total space is divided into four regions. Consider a Cartesian coordinate system (x, y, z) with unit vectors $\hat{x}$, $\hat{y}$ and $\hat{z}$. We take a TE$e^{i\omega t}$-monochromatic plane wave in free space with its wave vector $\vec{k}_0 = \hat{y}k_y + \hat{z}k_z$ in y-z plane, where $k_0 = \omega\sqrt{\mu_0\varepsilon_0}$ and $k_z = \sqrt{k_0^2 - k_x^2}$. In the case of TM wave, similar features and results can be obtained, which can be easily shown by using the duality principle.

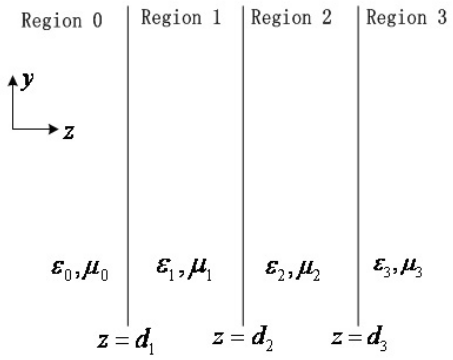

Figure 1. Geometry of the problem: TE wave interaction with the paired slabs.

For a TE plane wave in region 0, $E_x = E_0 e^{ik_z z + ik_y y}$, incident on the paired slabs, the total field in region l can be written as

$$\begin{aligned} E_{lx} &= \left(E_l^+ e^{ik_{lz}z} + E_l^- e^{-ik_{lz}z}\right) e^{ik_y y} \\ H_{ly} &= \frac{k_{lz}}{\omega\mu_l}\left(E_l^+ e^{ik_{lz}z} + E_l^- e^{-ik_{lz}z}\right) e^{ik_y y} \\ H_{lz} &= \frac{-k_y}{\omega\mu_l}\left(E_l^+ e^{ik_{lz}z} + E_l^- e^{-ik_{lz}z}\right) e^{ik_y y} \end{aligned} \tag{1}$$

where the amplitude E_l^+ represents the wave components that propagate along the positive z direction in region l, and E_l^- represents those with a velocity in the negative z direction. At $z = d_1, d_2, d_3$, the boundary conditions require that E_x and H_y be continuous. We can obtain

$$E_l^+ e^{ik_{lz}d_{l+1}} + E_l^- e^{-ik_{lz}d_{l+1}} = E_{l+1}^+ e^{ik_{(l+1)z}d_{l+1}} + E_{l+1}^- e^{-ik_{(l+1)z}d_{l+1}} \tag{2}$$

$$E_l^+ e^{ik_{lz}d_{l+1}} - E_l^- e^{-ik_{lz}d_{l+1}} = p_{l(l+1)}\left[E_{l+1}^+ e^{ik_{(l+1)z}d_{l+1}} - E_{l+1}^- e^{-lk_{(l+1)z}d_{l+1}}\right] \tag{3}$$

where

$$p_{l(l+1)} = \frac{\mu_l k_{(l+1)z}}{\mu_{l+1} k_{lz}} \tag{4}$$

The reflection coefficient $R = E_0^-/E_0^+$ can be obtained by (2) and (3) for $E_3^- = 0$. The reflection coefficient of the closed-form solution can be written as [13]

$$R = \frac{\left(\begin{array}{r} R_{01} + R_{12}e^{i2k_{1z}(d_2-d_1)} + R_{23}e^{i2k_{1z}(d_2-d_1)}e^{i2k_{2z}(d_3-d_2)} \\ +R_{01}R_{12}R_{23}e^{i2k_{2z}(d_3-d_2)} \end{array}\right) e^{i2k_{0z}d_1}}{\left(\begin{array}{r} 1 + R_{01}R_{12}e^{i2k_{1z}(d_2-d_1)} + R_{01}R_{23}e^{i2k_{1z}(d_2-d_1)}e^{i2k_{2z}(d_3-d2)} \\ +R_{12}R_{23}e^{i2k_{2z}(d_3-d_2)} \end{array}\right)} \tag{5}$$

where

$$R_{l(l+1)} = \frac{1 - p_{l(l+1)}}{1 + p_{l(l+1)}} \tag{6}$$

Through analyzing expression (5), we can get the conditions for zero reflection of the paired slabs,

$$R_{01} = R_{12} = R_{23} = 0 \tag{7}$$

or

$$\begin{cases} R_{l(l+1)} = 0 & \text{one of 0,1,2} \\ R_{l(l+1)} = \infty & \text{else} \end{cases} \tag{8}$$

or

$$\begin{cases} R_{12} = \infty \\ R_{01}R_{23} = -1 \\ k_{1z}(d_2 - d_1) = k_{2z}(d_3 - d_2) \end{cases} \tag{9}$$

The condition (7) means that constitutive parameters of all regions are the same media, so there is no reflection in nature. The condition (8) shows that region l and region $l+1$ are the same, while the values of their permeability are opposite to the other regions, like a double negative (DNG) slab in the air. The condition (9) exhibits that region 1 and region 2 have the opposite permeability, region 0 and region 3 are filled with the same media, and at the same time, it requires that slab thicknesses should satisfy Equation (9).

3. TRANSPARENCY OF PAIRING AN ENG SLAB WITH A MNG SLAB

It is well known that no waves can propagate in a single slab with one negative constitutive parameter and one positive constitutive parameter. However, pairing an ENG slab with a MNG slab in the air can exhibit salient features, such as zero reflection, only need to satisfy the condition (9). For a pair of an ENG slab and a MNG slab in the air, the zero reflection conditions given in (9) can be reduced to a simple form,

$$\begin{cases} \mu_1\varepsilon_1 - D^2\mu_2\varepsilon_2 = \dfrac{k_y^2(1-D^2)}{\omega^2} \\ \mu_1 + \mu_2 D = 0 \end{cases} \tag{10}$$

where

$$D = \frac{d_3 - d_2}{d_2 - d_1} \tag{11}$$

The latest conditions in general depend on the value of k_y, so the transparency of such paired slabs is related to a particular angle of incidence of the TE wave. However, when the thickness of ENG slab is the same as that of MNG slab, the transparency of such paired slabs is independent of the angle of incidence. The typical structure is shown

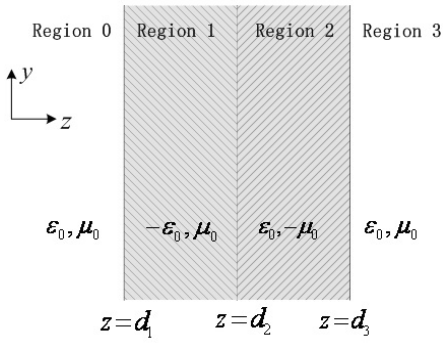

Figure 2. Geometry of pairing an ENG slab with a MNG slab.

in Fig. 2, where $d_3 = 2d_2 - d_1$. According to the analysis of Section 2, we know that waves can propagate through the paired slabs without any reflection. At the same time, the electric fields in any region can be obtained by the use of propagation matrices, which can be deduced by the boundary conditions (2) and (3).

$$\begin{bmatrix} E_1^+ \\ E_1^- \end{bmatrix} = \frac{E_0}{2}(1+p_{10}) \begin{bmatrix} e^{-1(k_{1z}-k_{0z})d_1} & R_{10}e^{-i(k_{1z}+k_{0z})d_1} \\ R_{10}e^{i(k_{1z}+k_{0z})d_1} & e^{i(k_{1z}-k_{0z})d_1} \end{bmatrix} \begin{bmatrix} 1 \\ 0 \end{bmatrix} \quad (12)$$

$$\begin{bmatrix} E_2^+ \\ E_2^- \end{bmatrix} = \frac{1}{2}(1+p_{21}) \begin{bmatrix} e^{-1(k_{2z}-k_{1z})d_2} & R_{21}e^{-i(k_{2z}+k_{1z})d_2} \\ R_{21}e^{i(k_{2z}+k_{1z})d_2} & e^{i(k_{2z}-k_{1z})d_2} \end{bmatrix} \begin{bmatrix} E_1^+ \\ E_1^- \end{bmatrix} \quad (13)$$

$$\begin{bmatrix} T \\ 0 \end{bmatrix} E_0 = \frac{1}{2}(1+p_{32}) \begin{bmatrix} e^{-1(k_{3z}-k_{2z})d_3} & R_{32}e^{-i(k_{3z}+k_{2z})d_3} \\ R_{32}e^{i(k_{3z}+k_{2z})d_3} & e^{i(k_{3z}-k_{2z})d_3} \end{bmatrix} \begin{bmatrix} E_2^+ \\ E_2^- \end{bmatrix} \quad (14)$$

where

$$R_{(l+1)l} = \frac{1-p_{(l+1)l}}{1+p_{(l+1)l}} = -R_{l(l+1)} \quad (15)$$

In order to observe the field distributions in every region, we have computed propagating wave patterns for such paired slabs when $E_0 = 1$, $d_1 = 100\,\text{mm}$, $d_2 = 200\,\text{mm}$ and $d_3 = 300\,\text{mm}$. At the frequency of 1 GHz, the real part and image part of electric filed patterns are illustrated in Fig. 3, so do the amplitude and phase of electric field. The corresponding magnetic components are shown in Fig. 4. In Fig. 3 and Fig. 4, we clearly see that the values of electric and magnetic fields at the front face of the pair are the same as that at the back face, including the real and imaginary parts. Fig. 3(d) shows that there is no phase change at back face comparing to the phase at the front face of the pair, although there are minor changes within such

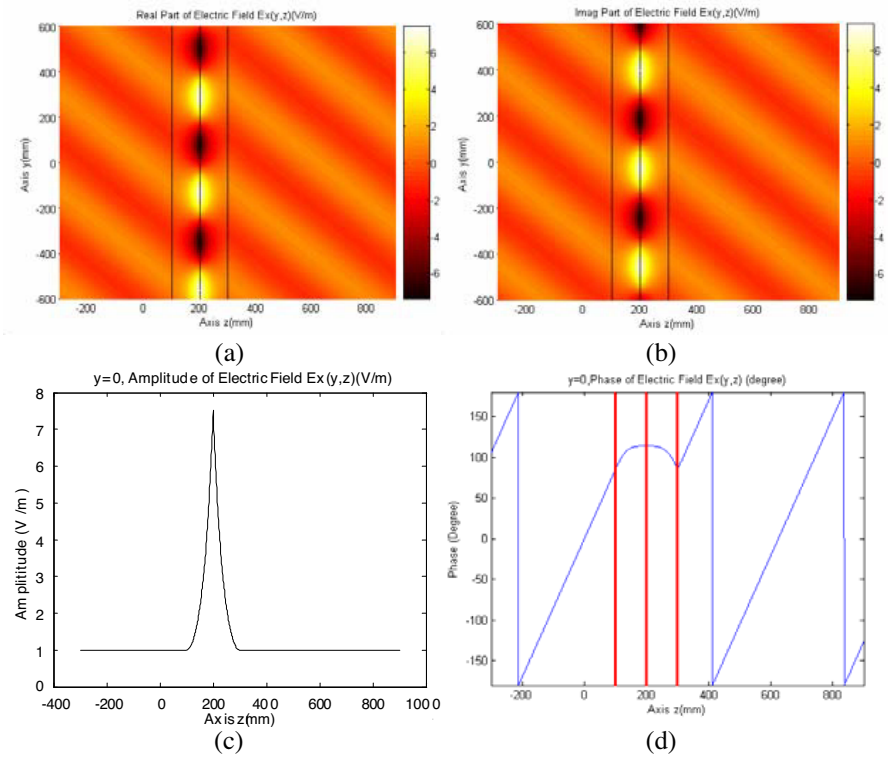

Figure 3. Electric field patterns of propagating waves within and outside the paired slabs when the frequency is 1 GHz and $d_1 = 100\,\text{mm}$, $d_2 = 200\,\text{mm}$ and $d_3 = 300\,\text{mm}$, (a) the real part, (b) the imagine part, (c) the amplitude, (d) the phase.

paired slabs. It is different form wave interaction with a LHM slab for the amplification of propagating wave in amplitude.

The electric fields are symmetrical in the paired slabs with respect to the axis $z = 200\,\text{mm}$, which is the interface of ENG slab and MNG slab. The magnetic field component H_y also is symmetrical, while H_z is anti-symmetrical. These results obtained are consistent with Maxwell boundary conditions — at the interface, the tangential components of electrical field E_x and magnetic field H_y are continuous, while normal B is continuous, which gives rise to the anti-symmetry of H_z inside the paired slabs.

Figure 5 illustrates the distribution of the real part (a) of the Poynting vector inside and outside the paired slabs and the amplitude (b) along the line $y = 0\,\text{mm}$. Here we see the complete flow of power

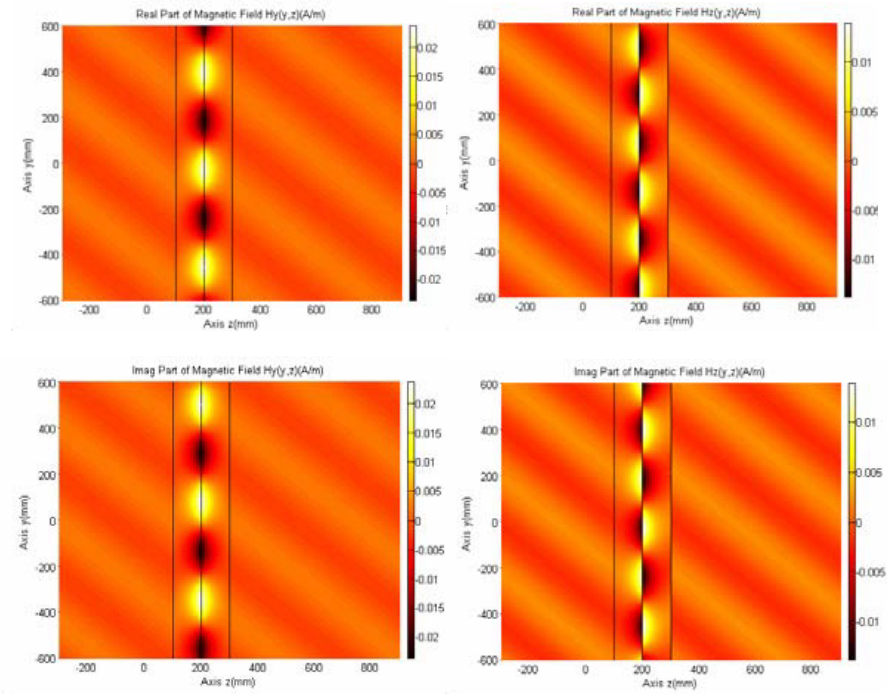

Figure 4. Magnetic field patterns of propagating waves within and outside the paired slabs when the frequency is 1 GHz and $d_1 = 100\,\text{mm}$, $d_2 = 200\,\text{mm}$ and $d_3 = 300\,\text{mm}$. The left figures are H_y component and the right figures are H_z components distributions, indicating the real and imaginary parts from the top to the bottom.

through the paired of slabs, while each of the ENG and MNG slabs by itself would not have allowed incident power to go through. Note that extremely high power densities appear at the interface of ENG slab and MNG slab, however, the energy conservation is not violated since the power flows in ENG slab and MNG slab have the same amplitude but opposite directions.

For evanescent waves, the paired slabs can also cancel the decay along $+z$ direction. We shall notice that evanescent waves are enhanced in ENG slab and decay in MNG slab, which yields the same value of electric field at front and back faces of paired slabs. In order to observe the field distributions of evanescent waves, the computational domain is chosen as $-250 \leq y \leq 250$ and $0 \leq z \leq 500$ (unit: mm), while the dimensions and parameters of paired slabs are the same as that of paired slabs used in computing propagating wave. The simulation

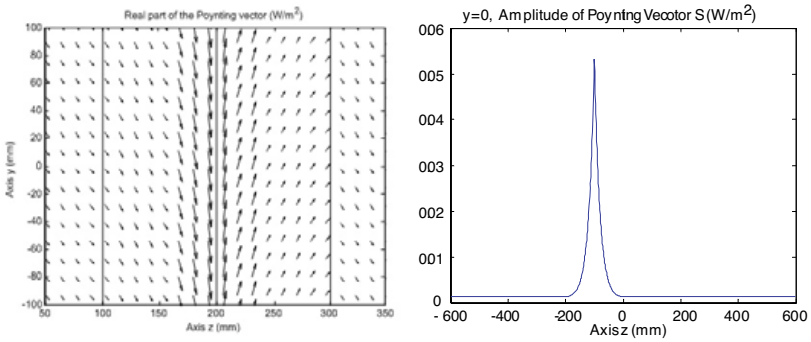

(a) (b)

Figure 5. Distribution of the real part (a) of the Poynting vector inside and outside the paired slabs and the amplitude (b) along the line $y = 0\,\text{mm}$.

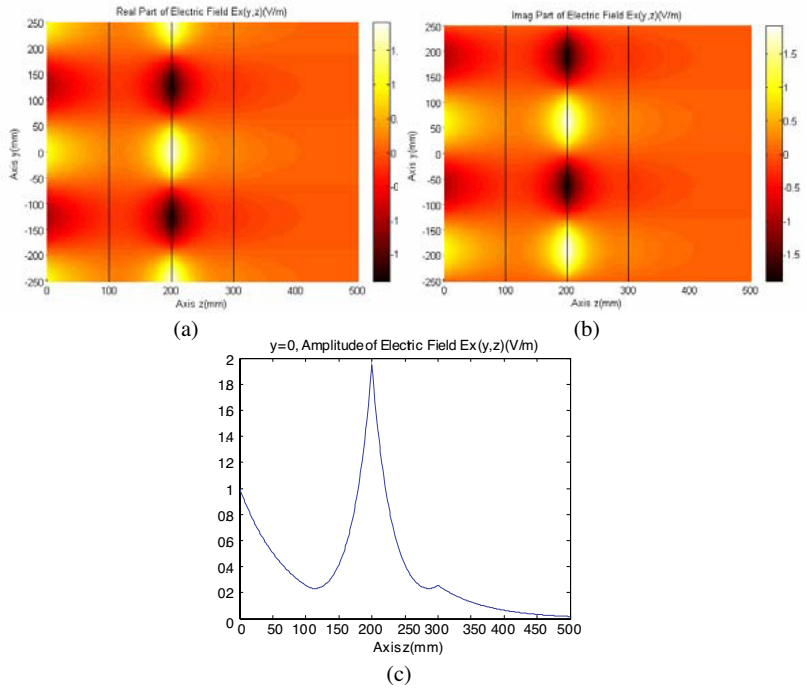

(a) (b)

(c)

Figure 6. Electric field patterns of evanescent waves within and outside the paired slabs when the frequency is 1 GHz and $d_1 = 100\,\text{mm}$, $d_2 = 200\,\text{mm}$ and $d_3 = 300\,\text{mm}$, (a) the real part, (b) the imaginary part, (c) the amplitude along the line $y = 0$.

results show that the paired slabs are transparent for evanescent waves, shown in Fig. 6. The amplitudes are the same at the front and back faces of the paired slabs, while there is no phase change within slabs for evanescent waves. The most interesting thing is the behaviors of waves at the interfaces $z = 100\,\text{mm}$ and $z = 300\,\text{mm}$, which is worthwhile for further study.

4. CONCLUSIONS

Through an exact analysis, we have shown the conditions of zero reflection for paired slabs, which is constituted of an ENG slab and a MNG slab. Although wave interaction with each of these slabs alone leads to predictable results, a pair of such ENG and MNG slabs is transparent for propagating wave and evanescent wave. The field distributions of propagating and evanescent waves inside and outside such paired slabs have been illustrated separately. The Poynting vector inside and outside the paired slabs also are studied, the complete flow of power through the paired of slabs can be observed. Such transparency of the paired slabs, under some conditions, may be found important applications in some new microwave and optical devices.

REFERENCES

1. Veselago, V. G., "The electrodynamics of substances with simultaneously negative values of ε and μ," *Soviet Physics USPEKI*, Vol. 10, No. 4, 509–514, Jan.–Feb. 1968.
2. Smith, D. R., W. J. Padilla, D. C. Vier, et al., "Composite medium with simultaneously negative permeability and permittivity," *Physical Review Letters*, Vol. 47, No. 11, 2075–2084, Nov. 1999.
3. Pendry, J. B., A. J. Holden, D. J. Robins, and W. J. Stewart, "Magnetism from conductors and enhanced nonlinear phenomena," *IEEE Trans. Microw. Theory Tech.*, Vol. 47, No. 11, 2075–2048, Nov. 1999.
4. Caloz, C. and T. Itoh, "Novel microwave devices and structures based on the transmission line approach of meta-materials," *IEEE MTT-S International Microwave Symposium Digest*, Vol. 1, 195–198, 8–13 June 2003.
5. Liang, L., B. Li, S.-H. Liu, and C.-H. Liang, "A study of using the double negative structure to enhance the gain of rectangular waveguide antenna arrays," *Progress In Electromagnetics Research*, PIER 65, 275–286, 2006.

6. Hamid, A.-K., "Axially slotted antenna on a circular or elliptic cylinder coated with metamaterials," *Progress In Electromagnetics Research*, PIER 51, 329–341, 2005.
7. Antoniades, M. A. and G. V. Eleftheriades, "Compact linear lead/lag metamaterial phase shifters for broadband applications," *IEEE Antennas and Wireless Propagation Letters*, Vol. 2, 2003.
8. Kuo, T.-N., S.-C. Lin, and C. H. Chen, "Compact ultra-wideband bandpass filters using composite microstrip-coplanar-waveguide sturcture," *IEEE Transactions on Microwave Theory and Techniques*, 1–7, 2006.
9. Caloz, C., A. Sanada, and T. Itoh, "A novel composite right-/left-handed coupled-line directional coupler with arbitrary coupling level and broad bandwidth," *IEEE Transaction on Microwave Theory and Techniques*, Vol. 52, No. 3, March 2004.
10. Sharma, R., T. Chakravarty, S. Bhooshan, and A. B. Bhattacharyya, "Design of a novel 3db microstrip backward wave coupler using defected ground structure," *Progress In Electromagnetics Research*, PIER 65, 261–273, 2006.
11. Fredkin, D. R. and A. Ron, "Effectively left-handed (negative index) composite material," *Applied Physics Letters*, Vol. 81, No. 10, September 2002.
12. Alù, A. and N. Engheta, "Pairing an epsilon-negative slab with a mu-negative slab: resonance, tunneling and transparency," *IEEE Transactions on Antennas and Propagation*, Vol. 51, No. 10, October 2003.
13. Kong, J. A., "Electromagnetic wave interaction with stratified negative isotropic media," *Progress In Electromagnetics Research*, PIER 35, 1–52, 2002.